PLoS one

[11C]flumazenil Binding Is Increased in a Dose-Dependent Manner with Tiagabine-Induced Elevations in GABA Levels

W. Gordon Frankle[1,2]*, Raymond Y. Cho[1], N. Scott Mason[2], Chi-Min Chen[1], Michael Himes[1], Christopher Walker[1], David A. Lewis[1,3], Chester A. Mathis[2], Rajesh Narendran[1,2]

1 Department of Psychiatry, University of Pittsburgh, Pittsburgh, Pennsylvania, United States of America, 2 Department of Radiology, University of Pittsburgh, Pittsburgh, Pennsylvania, United States of America, 3 Department of Neuroscience, University of Pittsburgh, Pittsburgh, Pennsylvania, United States of America

Abstract

Evidence indicates that synchronization of cortical activity at gamma-band frequencies, mediated through GABA-A receptors, is important for perceptual/cognitive processes. To study GABA signaling in vivo, we recently used a novel positron emission tomography (PET) paradigm measuring the change in binding of the benzodiazepine (BDZ) site radiotracer [11C]flumazenil associated with increases in extracellular GABA induced via GABA membrane transporter (GAT1) blockade with tiagabine. GAT1 blockade resulted in significant increases in [11C]flumazenil binding potential (BPND) over baseline in the major functional domains of the cortex, consistent with preclinical studies showing that increased GABA levels enhance the affinity of GABA-A receptors for BDZ ligands. In the current study we sought to replicate our previous results and to further validate this approach by demonstrating that the magnitude of increase in [11C]flumazenil binding observed with PET is directly correlated with tiagabine dose. [11C]flumazenil distribution volume (V_T) was measured in 18 healthy volunteers before and after GAT1 blockade with tiagabine. Two dose groups were studied (n = 9 per group; Group I: tiagabine 0.15 mg/kg; Group II: tiagabine 0.25 mg/kg). GAT1 blockade resulted in increases in mean (± SD) [11C]flumazenil V_T in Group II in association cortices (6.8±0.8 mL g−1 vs. 7.3±0.4 mL g−1; p = 0.03), sensory cortices (6.7±0.8 mL g−1 vs. 7.3±0.5 mL g−1; p = 0.02) and limbic regions (5.2±0.6 mL g−1 vs. 5.7±0.3 mL g−1; p = 0.03). No change was observed at the low dose (Group I). Increased orbital frontal cortex binding of [11C]flumazenil in Group II correlated with the ability to entrain cortical networks (r = 0.67, p = 0.05) measured via EEG during a cognitive control task. These data provide a replication of our previous study demonstrating the ability to measure in vivo, with PET, acute shifts in extracellular GABA.

Introduction

Accumulating evidence indicates that synchronization of cortical neuronal activity at gamma-band frequencies (30–80 Hz), mediated through GABA-A receptor transmission, is important for various types of perceptual [1,2,3] and cognitive processes [4,5]. In order to assess the relationship between changes in gamma band power and extracellular GABA levels, we recently using a novel positron emission tomography (PET) brain-imaging paradigm to measure the in vivo binding of the benzodiazepine (BDZ) site specific radiotracer [11C]flumazenil [6] at baseline and in the context of elevated GABA levels induced via blockade of the GABA membrane transporter (GAT1) with tiagabine (Gabitril®) [7]. Preclinical work suggests that increased GABA levels enhance the

affinity of GABA-A receptors for BDZ ligands via a conformational change (termed the 'GABA-shift') [8,9,10]; such an increase in affinity of GABA-A receptors should be detected as an increase in the binding of a GABA-A BDZ-receptor site-specific PET radioligand. In our study, GAT1 blockade resulted in significant increases in [11C]flumazenil binding potential (BP_{ND}) over baseline in brain regions representing the major functional domains of the cerebral cortex and this increase strongly predicted (r = 0.85, p = 0.015) the ability to entrain cortical networks, measured via EEG gamma synchrony during a cognitive control task in these same subjects [7]. These findings are consistent with the results of experimental models [11,12] as well as preclinical studies [13,14,15] suggesting that GABA-A receptor-mediated transmission is required for the induction of gamma network oscillations.

The aim of the current study was to replicate our previous results and to further validate the methods by demonstrating that the magnitude of increase in [¹¹C]flumazenil binding observed with PET is directly correlated with the degree of GABA increase. The refinement and validation of the PET methodology described previously would provide a unique ability to measure changes in extracellular GABA levels in vivo; examine the relationship between GABA neurotransmission, oscillatory activity and cognition; and to explore differences between control and patient populations in the degree of extracellular GABA increase in response to a standardized level of GAT1 blockade. Moreover, if abnormalities in GABA transmission exist in psychiatric disorders as suggested by recent studies in schizophrenia [16] and major depression [17], this technique could be employed in the process of developing new pharmacologic compounds with the target of increasing cortical GABA levels. Eighteen healthy volunteers underwent two [¹¹C]flumazenil PET scans on the same day, baseline and 60 minutes after administration of oral tiagabine; nine subjects received a dose of 0.15 mg/kg and nine subjects received a dose of 0.25 mg/kg. We hypothesized that the increase in [¹¹C]flumazenil binding after the administration of tiagabine will occur in a dose-dependent manner.

Materials and Methods

Human Subjects

The study was approved by the Institutional Review Board of the University of Pittsburgh Medical Center. Eighteen healthy volunteers provided written, informed, consent and participated in this study in two dose groups (Group I: tiagabine 0.15 mg/kg, age 24±3 years, range 21 to 29, 4M/5F; Group II: tiagabine 0.25 mg/kg, age 30±11 years, range 19 to 48, 5M/4F; with these and subsequent values given as mean ± SD). The absence of pregnancy, medical, neurological and psychiatric history (including alcohol and drug abuse) was assessed by history, review of systems, physical examination, routine blood tests including pregnancy test, urine toxicology and EKG. Subjects provided written informed consent after receiving an explanation of the study.

PET protocol

All subjects were studied twice with [¹¹C]flumazenil on the same day. On the study day an arterial catheter was inserted in the radial artery, after completion of the Allen test and infiltration of the skin with lidocaine, for blood sampling and a venous catheter was inserted in a forearm vein for radiotracer injection. First, a baseline PET scan was performed. The baseline scan was followed by oral administration of tiagabine (Group I 0.15 mg/kg; Group II 0.25 mg/kg) with the second PET scan beginning 60 minutes post-tiagabine administration. Calculated tiagabine dose was rounded to the nearest even number to prevent tablet splitting (lowest dosage form is a 2 mg tablet).

The scanning protocol was identical for all scans. PET imaging was performed with the ECAT EXACT HR+ (Siemens/CTI, Knoxville, TN). A 10 min transmission scan was obtained prior to each radiotracer injection for attenuation correction of the emission data. [¹¹C]Flumazenil was produced via a modification of published procedures [18]. Twenty mCi or less of high specific activity [¹¹C]flumazenil was injected i.v. over 30 sec. Emission data were collected in the 3D mode for 90 min as 19 successive frames of increasing duration (4×15 s, 3×1 min, 3×2 min, 2×5 min, 7×10 min). Subjects were allowed to rest outside of the camera for 30–60 min between the two injections. Subjects remained in the Montefiore University Hospital Clinical and Translational Research Center overnight after the PET scans to monitor for any side effects of tiagabine administration. Adverse effects observed in this study included sedation (mild to moderate) and ataxia (mild) and resolved completely within 4 hours of the scan.

Input function measurement

Following radiotracer injection, arterial samples were collected manually approximately every 6 s for the first two min and thereafter at longer intervals. A total of 35 samples were obtained per scan. Following centrifugation (2 min at 12,500 rpm, Spectrafuge 16M), plasma was collected in 200 µL aliquots and activities were counted in a gamma counter (Packard Biosciences).

To determine the plasma activity representing unmetabolized parent compound, seven samples (collected at 2, 5, 15, 30, 45, 75 and 90 min) were further processed via aqueous/organic extraction [19] to measure the fractional concentrations of hydrophilic metabolites and unchanged (lipophilic) [¹¹C]flumazenil. The seven measured, unmetabolized fractions were fitted to the sum of one exponential plus a constant and this function was used to interpolate values between the measurements.

The input function was calculated as the product of total counts and interpolated unmetabolized fraction at each time point. The measured input function values were fitted to a sum of three exponentials from the time of peak plasma activity and the fitted values were used as the input to the kinetic analysis. The clearance of the parent compound (L/h) was calculated as the ratio of the injected dose to the area under the curve of the input function [20].

For the determination of the plasma free fraction (f_P), triplicate aliquots of plasma collected prior to injection were mixed with the radiotracer, pipetted into ultrafiltration units (Amicon Centrifree; Bedford, MA) and centrifuged at room temperature (30 min at 6000 rpm). At end of centrifugation, the plasma and ultrafiltrate activities were counted (Packard Biosciences), and f_P was calculated as the ratio of activity in the ultrafiltrate to total activity [21]. Triplicate aliquots of saline solution mixed with the radiotracer were also processed, to determine the filter retention of the free tracer.

MRI acquisition and segmentation procedures

To provide an anatomical framework for analysis of the PET data, MRI scans were obtained using a 1.5 T GE Medical Systems (Milwaukee, WI) Signa Scanner. A 3D spoiled gradient recalled sequence was acquired in the coronal plane using parameters that were optimized for maximal contrast among gray matter, white matter, and CSF. The scalp and calvarium were removed from the SPGR MR images, to facilitate MR/PET coregistration, using a manual in-house stripping technique. MRI segmentation was performed using the FAST automated segmentation tool [22] implemented in the FMRIB Software Library, v4.0 [23].

Image analysis

PET data were reconstructed using filtered back-projection (Fourier rebinning/2D backprojection, 3 mm Hann filter) and corrected for photon attenuation (⁶⁸Ge/⁶⁸Ga rods), scatter [24], and radioactive decay. Reconstructed image files were then processed with the image analysis software MEDx (Sensor Systems, Inc., Sterling, Virginia) with the PET-MR image alignment performed using the SPM2 package (www.fil.ion.ucl.ac.uk/spm). PET data were inspected for subject motion and inter-frame motion was corrected using the realign procedure within SPM2, if necessary.

Regions of interest (ROIs) were drawn on each individual's MRI according to criteria derived from brain atlases [25,26] and applied to the coregistered dynamic PET data to generate regional time-activity curves. Three functionally-based cortical ROIs were obtained as weighted averages of component ROIs: Association Cortex (dorsolateral prefrontal, orbital frontal, medial prefrontal, anterior cingulate), Sensory Cortex (parietal, occipital), and the limbic Medial Temporal Lobe (MTL; amygdala, hippocampus, enterorrhinal ctx and parahippocampal gyrus).

For the neocortical regions, "large" regions were first drawn to delineate the boundaries of the ROIs. Within these regions, only the voxels classified as gray matter were used to measure the activity distribution. Sampled volumes of the neocortical regions (n = 6) were as follows: dorsolateral prefrontal cortex (DLPFC, 19390±2899 mm^3), orbito-frontal cortex (OFC, 10260±2448 mm^3), medial prefrontal cortex (MPFC, 5001±1660 mm^3), anterior cingulate cortex (ACC, 2587±686 mm^3), parietal cortex (PC, 74583±13081 mm^3), and occipital cortex (OC, 49286±7651 mm^3).

Because of the mixture of gray and white matter in the structures of the MTL, the segmentation-based approach was not used for the component ROIs, and the boundaries of these regions were identified by anatomical criteria. These regions (n = 4) included amygdala (AMY, 2410±404 mm^3), hippocampus (HIP, 4729±877 mm^3), entorhinal cortex (ENT, 960±243 mm^3), and parahippocampal gyrus (PHG, 6021±1382 mm^3).

For bilateral regions, right and left values were averaged. The contribution of plasma total activity to the regional activity was calculated assuming a 5% blood volume in the regions of interest [27] and tissue activities were calculated as the total regional activities minus the plasma contribution.

Derivation of distribution volumes

We denote here the outcome variables using the consensus nomenclature for in vivo imaging of reversibly binding radioligands [28]. Derivation of [^{11}C]flumazenil regional tissue distribution volume (V_T, mL g^{-1}) was performed with kinetic modeling using the arterial input function and an unconstrained two tissue compartment model (2TC model). V_T, which is equal to the ratio of tissue to plasma parent activity at equilibrium, was derived as $K_1/k_2(1+k_3/k_4)$, where K_1 (ml g^{-1} min^{-1}) and k_2 (min^{-1}) are the unidirectional fractional rate constants governing the transfer into and out of the brain, respectively, and k_3 (min^{-1}) and k_4 (min^{-1}) are the unidirectional fractional rate constants governing the association and dissociation of [^{11}C]flumazenil to and from the BZD-site, respectively [29,30,31]. Kinetic parameters were derived by nonlinear regression using a Levenberg-Marquart least-squares minimization procedure [32] implemented in MATLAB (The Math Works, Inc., South Natick, MA), as previously described [30]. Given the unequal sampling over time (increasing frame acquisition time from the beginning to the end of the study), the least-squares minimization procedure was weighted by the frame acquisition time.

In previous studies, including our own [7], the pons has been used as the region of reference as activity in this region has been reported to represent predominantly nonspecific binding [21,31,33]. However, postmortem studies [34,35,36] as well as previous receptor imaging studies [20], including unpublished imaging data from our lab in humans, have demonstrated significant (up to 60%) of the signal from the pons is due to specific binding. While in our previous study tiagabine administration did not alter the pons V_T (equilibrium nonspecific binding, V_{ND}) since the current study compared two dose of tiagabine we elected to utilize the V_T as our main outcome measure. However, for the purpose of comparison, we include the [^{11}C]flumazenil

binding potential relative to the total plasma concentration of [^{11}C]flumazenil (BP_P, mL g^{-1}) derived as the difference between V_T in the ROI and V_{ND} (pons V_T). The relationship between BP_P and BDZ receptor parameters is given by $BP_P = f_P * B_{max}/K_D$, where B_{max} is GABA-A BDZ-receptor density, $1/K_D$ is the in vivo affinity of [^{11}C]flumazenil for the GABA-A BDZ-receptor and f_P is the fraction of the radiotracer unbound to protein in the plasma.

Derivation of Affinity Shift via Linear Regression Analysis

Lassen et al [37] demonstrated the ability to estimate the fractional change in binding potential (ΔBP) as the slope of the linear regression of the difference in V_T across conditions vs. the baseline V_T for cases where only the distribution volume and not the binding potential can be measured. In this study the linear regression of ($V_{T\ baseline}$ - $V_{T\ post\ tiagabine}$) vs. $V_{T\ baseline}$ results in a line with a slope of ΔBP and an x-intercept of V_{ND}. Assuming the affinity shift secondary to increased GABA levels is the same across all regions the shift in affinity is equal to 1- ΔBP, or 1 – slope of the plot of ($V_{T\ baseline}$ - $V_{T\ post\ tiagabine}$) vs. $V_{T\ baseline}$. In each subject the percent change in affinity as well as V_{ND} was determined via this method using the values of V_T from the ten ROIs examined in the study (DLPFC, OFC, MPFC, ACC, PC, OC, AMY, HIP, ENT, and PHG) pre- and post-tiagabine administration.

Electrophysiology and Cognitive Task

In all subjects the electrophysiology study was performed approximately 1 week prior to the PET scans. The Preparing to Overcome Prepotency (POP) task is a cued stimulus-response reversal paradigm that requires increases in cognitive control to overcome prepotent response tendencies [38]. Trials proceeded in the following order: cue (a green or red square; 500 ms); delay period (1000 ms); probe (a white arrow pointing left or right; 1000 ms); and a variable inter-trial interval (1000–2000 ms). Cues indicated conditions requiring either low (green square) or high (red square) degrees of cognitive control. Over the delay period, subjects were required to maintain the trial-type information and prepare for a response to the upcoming probe. For low-control trials, subjects were required to respond in the direction of the arrow that followed (e.g., for a right-pointing arrow, press the right button); for the high-control trials, responses were required in the opposite direction (e.g., for a right-pointing arrow, press the left button). To reinforce the prepotency of the cue-probe mappings of the low-control trials, thereby increasing the control requirements during the high-control trials, 70% of the trials were low-control and the remaining 30% were high-control. Trial types were interleaved in pseudorandom order, with 8 blocks of 42 trials each.

During the POP task, EEG data were acquired using a 129 Ag-AgCl coated carbon fiber electrode Geodesic Sensor Net (EGI, Eugene, OR) with a sampling frequency of 250 Hz. Data were filtered on-line with a 0.1–100 Hz band pass hardware filter. Electrode impedances were kept below 50 kΩ. All channels were referenced to Cz. Epochs were defined as −400 to +1900 ms relative to the cue onset. Error trials and epochs containing artifacts were excluded (20 channels with amplitude range exceeding 200 μV within a segment and/or having 60 μV deviations between consecutive samples). Segments identified by these criteria were visually inspected prior to rejection. Blink and ECG artifacts were removed with ICA based detection and correction methods. Data were filtered off-line using an 1–100 Hz finite impulse response filter. The resulting data were submitted to final review using the above amplitude and gradient criteria and for 60 Hz line noise, with bad channel data being replaced by interpolation. Data were re-referenced to average reference [39].

Average segment counts for the high and low control conditions were 220 and 80, respectively.

Time-frequency analyses were carried out using Brain Vision Analyzer (Brain Products GmbH, Munich, Germany). The data were transformed using complex Morlet wavelet transforms, defined by $mo(x) = c \cdot exp(-x^2/2) \cdot exp(i\omega_0 x)$, with c = 7, using 20 frequency steps spanning 14–80 Hz. Wavelet transformed data were baseline corrected to a −300 to −100 ms pre-cue interval.

EEG analysis involved identifying frontal areas of peak induced (i.e., not time locked to stimulus) gamma activity differences between the high and low control conditions, with a focus on the delay period (500–1500 ms relative to cue onset) during which induced frontal gamma activity has been shown to modulate in accordance with cognitive control demands [38]. Activity from one representative electrode from each of the left and right frontal areas, respectively, was averaged to derive a spatially averaged measure for comparison to the PET data. The peak activity was in the gamma sub-band with central frequency 42 Hz in a left frontal region consisting of adjacent electrode locations E23, E24 and E27 (approximately AF3 and AF7, respectively, in the 10-10 system). This procedure resulted in one summary measure of frontal gamma activity for each subject, which were then compared to the individual measurements of tiagabine induced increase in [^{11}C]flumazenil binding by PET. Note that an experimenter blind to the PET data performed the determinations of these EEG measures of frontal gamma.

Statistical analysis

Between scan comparisons were assessed with a paired, two-tailed t-test with a significance level of 0.05. Baseline and post-tiagabine K_1 and V_T for the three functional cortical regions and V_{ND} (pons V_T) were compared using a two-tailed, paired t-test, with an uncorrected probability value of 0.05 selected as the significance level. For the analysis of the tiagabine-induced change in V_T in the component ROIs (n = 10) a univariate repeated-measures analysis of variance (RM ANOVA) with brain regions as the within-scan factor and condition (baseline or post-tiagabine) as the between-scan factor was used. Paired t-tests were performed,

when appropriate, to determine which regions accounted for significant effects observed in the RM ANOVA. The relationship between the PET scan outcome measures and the measurement of gamma-band power were analyzed with the Pearson product moment correlation coefficient after first confirming normal distribution of the data using the Kolmogorov-Smirnov test.

Results

PET scan parameters

No difference was observed in the injected dose, specific activity or injected mass of [^{11}C]flumazenil between the baseline and post-tiagabine scan in either group (Table 1). Tiagabine administration did not affect the plasma clearance of [^{11}C]flumazenil, [^{11}C]flumazenil plasma free fraction (f_P) or the distribution volume (V_T) of [^{11}C]flumazenil in the pons (Table 1).

Regional distribution volumes, K_1 values and BZD receptor availability

Dose Group I: Administration of 0.15 mg/kg tiagabine did not result in a significant change in V_T in any of the large cortical regions (these and subsequent values noted as mean ± standard deviation, p values for two-tailed, paired t-test unless otherwise stated); Association Cortex 7.6±0.6 mL g^{-1} vs. 7.7±0.4 mL g^{-1} (p = 0.84), Sensory Cortex 7.5±0.5 mL g^{-1} vs. 7.3±1.0 mL g^{-1} (p = 0.64) and limbic Medial Temporal Lobe (MTL) 5.9±0.5 mL g^{-1} vs. 5.9±0.3 mL g^{-1} (p = 0.86). Examination of V_T across the component ROIs revealed significant regional effect (RM ANOVA F = 186.3, df = 9, 8, p<0.0001), no region by condition interaction (RM ANOVA F = 0.51, df = 9, 8, p = 0.84) and no significant difference across conditions (RM ANOVA F = 0.008, df = 1, 16, p = 0.93), see Table 2.

Similarly, neither K_1 (Table 3) nor BP_P (Table 4) were changed with the 0.15 mg/kg dose of tiagabine. Examination of K_1 revealed a significant regional effect (RM ANOVA F = 265.4, df = 9, 8, p<0.0001), no region by condition interaction (RM ANOVA F = 0.47, df = 9, 8, p = 0.86) and no difference across conditions (RM ANOVA F = 1.3, df = 1, 16, p = 0.27). Examina-

Table 1. Demographic and scan data.

Parameter	Dose Group I			Dose Group II		
	Baseline	Post-tiagabine	p	Baseline	Post-tiagabine	p
N	9	9	-	9	9	-
Age	23.7±2.5	-	-	30.6±10.9	-	-
Gender	4M/5F	-	-	5M/4F	-	-
Ethnicity	1AA/7C/1H	-	-	3AA/6C	-	-
Tiagabine						
Dose (mg/kg)	-	0.14±0.01	-	-	0.24±0.01	-
Plasma level[1] (ng/mL)	-	141±55	-	-	291±69	-
Injected dose (mCi)	19.9±2.0	20.4±1.8	0.45	20.9±0.8	21.0±1.0	0.72
SA (Ci/mmoles)	1963±757	2007±693	0.89	1837±1048	2254±2068	0.55
Injected Mass (ug)	3.4±0.9	3.5±1.6	0.79	4.6±3.0	4.7±3.9	0.86
Free Fraction (f_P, %)	58.0%±7.6%	59.6%±6.1%	0.31	54.6%±7.8%	56.9%±5.2%	0.12
Clearance (L/h)	53±67	53±23	1.00	43±22	56±25	0.23
Pons V_T (or V_{ND} mL/g)	1.0±0.1	1.0±0.1	0.56	0.9±0.1	1.0±0.1	0.17

AA, African-American, AS, Asian, C, Caucasian. Significance level given is for a paired, two-tailed t-test.
[1]Plasma level take at the time of the scan.
doi:10.1371/journal.pone.0032443.t001

Table 2. Tiagabine-induced change in [11C]flumazenil V_T in control subjects.

Subdivision - Component ROIs	Dose Group I (0.15 mg/kg)					Dose Group II (0.25 mg/kg)				
	Baseline V_T	Post-tiagabine V_T	ΔV_T (%)	d	p	Baseline V_T	Post-tiagabine V_T	ΔV_T (%)	d	p
Association Cortex	**7.6±0.6**	**7.7±0.4**	**0.8±6.5**	**−0.07**	**0.84**	**6.8±0.8**	**7.3±0.4**	**9.3±11.4**	**−0.99**	**0.03**
-DLPFC	7.6±0.6	7.6±0.4	0.5±6.0	−0.03	0.92	6.7±0.8	7.2±0.4	9.5±11.2	−1.00	0.03
-Orbital Frt Ctx	7.5±0.7	7.5±0.6	0.4±7.8	−0.01	0.98	6.7±0.7	7.2±0.5	8.0±13.0	−0.82	0.11
-MPFC	8.0±0.6	8.1±0.5	1.0±7.0	−0.11	0.77	7.1±1.0	7.8±0.5	11.2±12.3	−0.92	0.02
-Ant. Cingulate Ctx	7.8±0.6	8.0±0.5	2.9±7.9	−0.38	0.36	7.2±0.8	7.7±0.5	7.5±11.3	−0.72	0.08
Sensory Cortex	**7.5±0.5**	**7.3±1.0**	**−1.9±14.9**	**0.26**	**0.64**	**6.7±0.8**	**7.3±0.5**	**9.7±10.8**	**−0.97**	**0.02**
-Parietal Ctx	7.3±0.4	7.4±0.4	0.8±8.1	−0.08	0.87	6.6±0.8	7.1±0.5	9.5±11.3	−0.88	0.03
-Occipital Ctx	7.7±0.6	7.4±1.5	−4.2±21.2	0.34	0.53	7.0±0.8	7.6±0.4	9.7±10.2	−1.06	0.02
Medial Temporal Lobe	**5.9±0.5**	**5.9±0.3**	**0.0±7.8**	**0.07**	**0.86**	**5.2±0.6**	**5.7±0.3**	**9.4±10.7**	**−1.02**	**0.03**
-Amygdala	5.9±0.6	5.8±0.4	−0.6±10.1	0.14	0.73	5.2±0.6	5.6±0.4	8.0±12.0	−0.79	0.11
-Hippocampus	6.0±0.5	5.9±0.3	−1.1±8.3	0.23	0.58	5.1±0.5	5.6±0.4	10.1±10.6	−1.15	0.02
-Entor. Ctx	5.6±0.4	5.6±0.3	0.9±7.9	−0.09	0.84	5.1±0.7	5.5±0.3	9.7±11.6	−0.83	0.03
-Parahippocampus	6.0±0.5	6.0±0.3	0.6±7.2	−0.03	0.93	5.4±0.7	5.8±0.3	9.4±10.6	−0.89	0.02

Values are Mean ± SD, in healthy controls (n = 9 per group); p is the significance level of the difference between the baseline and post-tiagabine scans in each group (paired t-test); d is the Cohen's effect size of this difference.
doi:10.1371/journal.pone.0032443.t002

tion of BP_P revealed a significant regional effect (RM ANOVA F = 186.4, df = 9, 8, p<0.0001), no region by condition interaction (RM ANOVA F = 0.51, df = 9, 8, p = 0.84) and no difference across conditions (RM ANOVA F = 0.05, df = 1, 16, p = 0.83).

Dose Group II: After the administration of 0.25 mg/kg tiagabine V_T increased significantly in the large cortical regions; Association Cortex 6.8±0.8 mL g^{-1} vs. 7.3±0.4 mL g^{-1} (p = 0.03), Sensory Cortex 6.7±0.8 mL g^{-1} vs. 7.3±0.5 mL g^{-1} (p = 0.02) and limbic Medial Temporal Lobe (MTL) 5.2±0.6 mL g^{-1} vs. 5.7±0.3 mL g^{-1} (p = 0.03). Examination of V_T across the component ROIs revealed a significant regional effect (RM ANOVA F = 118.9, df = 9, 8, p<0.0001), no region by condition interaction (RM ANOVA F = 0.42, df = 9, 8, p = 0.42) and a trend-level difference across conditions (RM ANOVA F = 4.0, df = 1, 16, p = 0.06). On a region-by-region basis, significant increases in all regions were seen post-tiagabine (Table 2) with the exception of the orbital prefrontal cortex (ORB, p = 0.11), anterior cingulate cortex (ACC, p = 0.08) and the amygdala (AMY, p = 0.11). No significant correlations between age or tiagabine plasma concentration and V_T increase were noted.

As observed in the lower dose group K_1 (Table 3) did not change significantly with the administration of 0.25 mg/kg of tiagabine; a significant regional effect (RM ANOVA F = 249.7, df = 9, 8, p<0.0001), no region by condition interaction (RM ANOVA F = 0.57, df = 9, 8, p = 0.82) and no difference across conditions (RM ANOVA F = 0.66, df = 1, 16, p = 0.43) were observed.

However, as opposed to the lower dose level, BP_P increased significantly in the large cortical regions with 0.25 mg/kg of tiagabine (Table 4); Association Cortex 5.9±0.7 mL g^{-1} vs. 6.4±0.4 mL g^{-1} (p = 0.05), Sensory Cortex 5.8±0.7 mL g^{-1} vs. 6.3±0.5 mL g^{-1} (p = 0.03) and limbic Medial Temporal Lobe (MTL) 4.3±0.6 mL g^{-1} vs. 4.7±0.3 mL g^{-1} (p = 0.04). Examination of BP_P across the component ROIs revealed a significant regional effect (RM ANOVA F = 118.9, df = 9, 8, p<0.0001), no region by condition interaction (RM ANOVA F = 0.42, df = 9, 8, p = 0.89) and a trend-level difference across conditions (RM ANOVA F = 3.31, df = 1, 16, p = 0.09).

Linear Regression Analysis

In Dose Group I, given the lack of change in V_T, the linear regression analysis did not result in meaningful data. In Dose Group II the average slope was −0.27±2.84 and the average x-intercept was 1.53±7.14 (n = 9 subjects). The affinity shift, calculated as 1 − slope, was 1.27±2.84, in other terms, on average, a 27% increase in affinity was observed across subjects in this dose group.

Electroencephalogram (EEG) induced gamma-band oscillations

To confirm our previous results which indicated that individuals with greater capacity to increase extracellular GABA levels post-tiagabine (a "GABA reserve") would exhibit enhanced frontal gamma-band oscillatory activity in the context of a task that taps cognitive control processes [7], all subjects underwent EEG measurement of frontal lobe gamma-band oscillations during the Preparing to Overcome Prepotency (POP) task [38]. Frontal cortical gamma-band power was measured in each individual during the delay period. Given that no change in [11C]flumazenil binding was noted in Dose Group I, it would not be expected to note an association between change in [11C]flumazenil binding and gamma band power; in fact this was confirmed (r = 0.12, p = 0.76). For Group II the association between gamma-band power and the ability to increase extracellular GABA levels was significant in the orbital frontal cortex (r = 0.67, p = 0.05; Figure 1) but in none of the other regions examined, although the directionality was the same across all regions. No relationship was observed between behavioral performance on the POP task and gamma-band power or change in [11C]flumazenil binding as all individuals performed at a high level on the task.

Discussion

The results of this study confirm our previous finding that acute increases in extracellular cortical GABA can be detected as an increase in binding of the BDZ-site specific radiotracer, [11C]flu-

Table 3. Tiagabine-induced change in [11C]flumazenil K_1 in control subjects.

Subdivision - Component ROIs	Dose Group I (0.15 mg/kg)				Dose Group II (0.25 mg/kg)			
	Baseline K_1	Post-tiagabine K_1	d	p	Baseline K_1	Post-tiagabine K_1	d	p
Association Cortex	**0.441±0.03**	**0.463±0.04**	**−0.66**	**0.18**	**0.405±0.06**	**0.421±0.05**	**−0.31**	**0.27**
-DLPFC	0.447±0.03	0.467±0.04	−0.57	0.22	0.407±0.06	0.424±0.05	−0.34	0.21
-Orbital Frt Ctx	0.429±0.03	0.452±0.04	−0.67	0.23	0.394±0.06	0.411±0.05	−0.36	0.22
-MPFC	0.452±0.04	0.477±0.04	−0.72	0.15	0.419±0.07	0.438±0.05	−0.32	0.14
-Ant. Cingulate Ctx	0.425±0.04	0.455±0.04	−0.77	0.08	0.408±0.06	0.434±0.06	−0.45	0.09
Sensory Cortex	**0.438±0.04**	**0.447±0.07**	**−0.17**	**0.73**	**0.412±0.05**	**0.425±0.05**	**−0.28**	**0.21**
-Parietal Ctx	0.443±0.04	0.468±0.04	−0.66	0.18	0.412±0.05	0.432±0.05	−0.40	0.08
-Occipital Ctx	0.429±0.05	0.428±0.10	0.02	0.96	0.408±0.05	0.419±0.04	−0.25	0.28
Medial Temporal Lobe	**0.308±0.03**	**0.332±0.04**	**−0.68**	**0.10**	**0.291±0.04**	**0.304±0.03**	**−0.40**	**0.17**
-Amygdala	0.316±0.04	0.331±0.03	−0.42	0.33	0.295±0.04	0.298±0.03	−0.09	0.75
-Hippocampus	0.310±0.03	0.332±0.04	−0.67	0.06	0.287±0.03	0.309±0.02	−0.78	0.03
-Entor. Ctx	0.270±0.04	0.294±0.03	−0.72	0.07	0.264±0.04	0.280±0.03	−0.50	0.16
-Parahippocampus	0.308±0.03	0.331±0.04	−0.63	0.10	0.293±0.04	0.311±0.03	−0.52	0.06

Values are Mean ± SD, in healthy controls (n = 9 per group); p is the significance level of the difference between the baseline and post-tiagabine scans in each group (paired t-test); d is the Cohen's effect size of this difference.
doi:10.1371/journal.pone.0032443.t003

mazenil. Moreover, these data indicate a dose-response relationship in the magnitude of the increase in [^{11}C]flumazenil binding and provide an estimate of the change in affinity at the BZD-site (27% increase) resulting in the increased binding. A critical assumption of this study is that systemic administration of tiagabine results in an acute, dose-dependent, increase in extracellular GABA. Tiagabine is a highly selective GAT1 blocker, without significant affinity for other receptors which, in humans, exhibits linear pharmacokinetics over the dose range of 2–24 mg with high oral bioavailability (90%) and peak plasma levels at approximately 1 hr post-dose [40]. In humans, tiagabine dose has been correlated to changes in brain GABA levels by the observation that there is a significant relationship between dose and reduction in seizure frequency [41] and through a microdialysis study in a single patient which found a 50% increase in hippocampal GABA levels with a 16 mg oral dose, occurring 1 hr post-dose and sustained for several hours [42]. Rodent microdialysis studies have shown that ip injection of tiagabine (11.5 and 21 mg/kg) increases extracellular GABA concentration ~200%–400% over basal levels in a dose-dependent manner,

Table 4. Tiagabine-induced change in [11C]flumazenil BP_P in control subjects.

Subdivision - Component ROIs	Dose Group I (0.15 mg/kg)					Dose Group II (0.25 mg/kg)				
	Baseline BP_P	Post-tiagabine BP_P	ΔBP_P (%)	d	p	Baseline BP_P	Post-tiagabine BP_P	ΔBP_P (%)	d	p
Association Cortex	**6.6±0.6**	**6.7±0.4**	**0.5±7.0**	**−0.02**	**0.95**	**5.9±0.7**	**6.4±0.4**	**9.5±12.7**	**−0.91**	**0.05**
-DLPFC	6.6±0.6	6.6±0.4	0.2±6.2	0.02	0.94	5.8±0.7	6.3±0.4	9.7±12.6	−0.91	0.05
-Orbital Frt Ctx	6.5±0.6	6.5±0.6	0.1±8.6	0.04	0.91	5.8±0.7	6.2±0.5	8.0±14.9	−0.70	0.17
-MPFC	7.0±0.5	7.1±0.5	0.7±7.6	−0.06	0.87	6.2±0.9	6.8±0.5	11.6±13.1	−0.87	0.03
-Ant. Cingulate Ctx	6.8±0.6	7.0±0.4	3.0±8.8	−0.34	0.41	6.3±0.8	6.7±0.6	7.4±12.8	−0.62	0.14
Sensory Cortex	**6.5±0.5**	**6.3±0.9**	**−2.5±17.1**	**0.30**	**0.60**	**5.8±0.7**	**6.3±0.5**	**10.0±11.8**	**−0.90**	**0.03**
-Parietal Ctx	6.3±0.4	6.4±0.4	0.5±9.3	−0.02	0.97	5.7±0.7	6.2±0.5	9.7±12.5	−0.81	0.04
-Occipital Ctx	6.7±0.6	6.3±1.5	−5.0±24.2	0.37	0.50	6.1±0.7	6.6±0.4	9.9±10.9	−0.99	0.02
Medial Temporal Lobe	**4.9±0.5**	**4.9±0.3**	**−0.5±8.2**	**0.14**	**0.71**	**4.3±0.6**	**4.7±0.3**	**9.7±11.6**	**−0.91**	**0.04**
-Amygdala	4.9±0.6	4.8±0.5	−1.3±10.5	0.19	0.61	4.4±0.5	4.6±0.3	8.0±13.0	−0.69	0.15
-Hippocampus	5.0±0.5	4.9±0.4	−1.8±8.7	0.28	0.43	4.2±0.5	4.6±0.3	10.6±11.2	−1.04	0.02
-Entor. Ctx	4.6±0.4	4.6±0.3	0.5±8.8	−0.01	0.98	4.2±0.7	4.6±0.3	10.3±13.5	−0.69	0.06
-Parahippocampus	5.0±0.5	5.0±0.4	0.3±7.9	0.03	0.93	4.5±0.6	4.8±0.3	9.7±11.7	−0.78	0.03

Values are Mean ± SD, in healthy controls (n = 9 per group); p is the significance level of the difference between the baseline and post-tiagabine scans in each group (paired t-test); d is the Cohen's effect size of this difference.
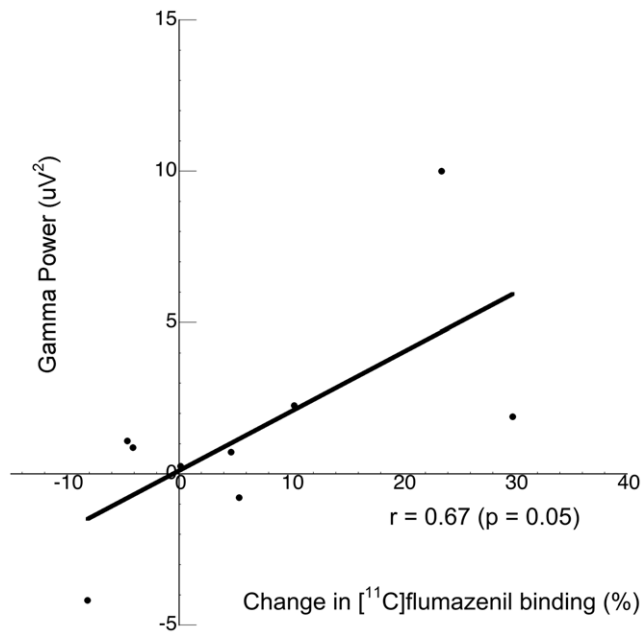doi:10.1371/journal.pone.0032443.t004

Figure 1. The ability to increase GABA levels in the orbito-frontal cortex, measured as the change in [^{11}C]flumazenil binding in response to GAT1 blockade, predicts (r = 0.67, p = 0.05) the ability to entrain cortical networks, measured via EEG gamma oscillations.
doi:10.1371/journal.pone.0032443.g001

peaking 40–60 minutes following injection [43,44] and after administration of tiagabine (1 mg/kg iv), a 2-fold increase in extracellular GABA levels was observed, reaching a maximum approximately 70 minutes post-tiagabine in vervet monkeys [45]. Taken together these preclinical studies support the assumption that extracellular GABA levels increase in a dose-dependent manner with tiagabine.

The principle underlying the hypothesis of a 'GABA-shift' is the enhancement in BDZ-receptor affinity for BDZ-site substrates resulting from increased GABA [9,10]. It is widely accepted that BDZs potentiate the effects of GABA at the GABA-A receptor and the reverse is true, increased GABA levels potentiate the binding of BDZs to the GABA-A receptor in a dose-dependent manner [9]. Some in vitro studies exploring this phenomenon indicate that it is specific to agonist drugs [46] while other in vitro studies were not able to demonstrate the GABA-shift, even with BDZ agonists [47]. Two preclinical studies have examined the effects of increasing GABA and GABAergic drugs on flumazenil binding in intact animals and both found results consistent with our findings. The first [48] demonstrated enhanced [^{3}H]flumazenil binding in vivo when mice were treated with either progabide (a GABA analog and agonist at the GABA-A receptor) or valproate, which increases brain GABA levels [49]. The second [8] measured the effects of three GABAergic drugs, aminooxyacetic acid (inhibitor of GABA transaminase, the enzyme that metabolizes GABA), gamma-vinyl GABA (GVG, irreversible GABA transaminase inhibitor) and valproate on [^{3}H]flumazenil binding. All three drugs resulted in acute increases in cortical GABA concentrations and specific binding of [^{3}H]flumazenil increased acutely across all brain regions, with all three drugs, with no change in nonspecific binding. These results, as well as those observed in our studies, suggest that while flumazenil acts as a benzodiazepine site antagonist in most settings it may also behave as a high affinity partial agonist with weak efficacy in others. This hypothesis is

consistent with studies showing flumazenil to be anxiolytic in some rodent models of anxiety [50] as well as in normals in stressful (public speaking) settings but not at baseline [51], to reduced benzodiazepine withdrawal symptoms in dependent subjects [52] and to enhance the GABA-A receptor mediated currents evoked by GABA [53].

The strengths of the present study include measurement of the arterial input function, allowing for the assessment of the effects of tiagabine on V_{ND} and f$_P$. While the absence of change in these variables post-tiagabine validates the use of either BP_P or BP_{ND} as an outcome measure, we chose to use V_T, derived via 2TC modeling, as our primary outcome measure. Our rationale for selecting V_T as the outcome measure in this study was the postmortem studies [34,35,36], previous receptor imaging study [20] and unpublished data from our lab, all of which demonstrate a significant degree of specific binding in the pons (up to 60%). We were concerned that differential effects of elevated GABA levels on [^{11}C]flumazenil specific binding in the pons would impact the comparison across tiagabine dose groups. Since we anticipated a greater increase in [^{11}C]flumazenil binding in the high dose group, specific binding within the pons would impact either BP_P or BP_{ND} to a greater degree in this group relative to the low dose group potentially obscuring group differences in tiagabine induced change in [^{11}C]flumazenil binding, despite the fact that, on average, no changes were seen in the pons V_T post tiagabine in either group. In fact, this is what we observed; as pons V_T is progressively included in the outcome measure there is a loss of significant differences likely secondary to elevations in pons V_T with tiagabine administration. Examination of V_T (Table 2), BP_P (Table 4) and BP_{ND} (data not shown) in the high dose group demonstrates a significant change in V_T, a trend-level change in BP_P, and no change in BP_{ND}.

In our previously published study we noted a relatively high variability in the percent change in [^{11}C]flumazenil binding across subjects. One factor we postulated may be involved in the variability was the timing of the PET scan relative to the administration of tiagabine [6]. In our initial study, we timed the PET scan such that scanning commenced at 30 min post dose to ensure the measurement occurred during the acute increase in GABA coinciding with the reported Tmax of the plasma concentration of tiagabine (45–60 min); however, microdialysis studies indicate GABA increases are sustained for several hours after oral administration of tiagabine. In the current study we increased the time between tiagabine administration and the start of PET scanning from 30 to 60 min, allowing for more consistent absorption of tiagabine across subjects. In addition we based the tiagabine dose on subject weight as opposed to using a standard, single, dose for each subject (as we did in our first study). Despite these changes in study design the variability in the percent change in [^{11}C]flumazenil binding was not significantly altered nor did we detect a correlation between tiagabine plasma level and change in [^{11}C]flumazenil binding (data not shown). In our first study we noted a significant increase in V_T across the ROIs used in this study (average increase in V_T of 13.7%±15.9%). This increase is comparable, albeit numerically larger, to that observed in Dose Group II, where we noted an average increase in V_T of 9.3%±10.9% across the 10 component ROIs listed in Table 2. Detecting differences between individuals with a psychiatric disorder and healthy controls may be challenging with this level of variability in the measurement; however, comparing the two groups in this study we noted the increase in [^{11}C]flumazenil V_T to be greater for Group II vs. Group I at a trend level (p = 0.06, RM ANOVA). In other words, relatively large between-dose differences can be detected with the current method (the average

increase in V_T for Dose Group I was 0.12%±9.7%) but more subtle differences in GABA availability may be difficult to detect without improvements in the methods to reduce the variability.

The goal of the present study was to validate our previous findings by demonstrating that the magnitude of increase in [^{11}C]flumazenil binding observed with PET is directly correlated with the degree of increase in extracellular GABA. We utilized increased tiagabine dose as a proxy for increased extracellular GABA levels since the only direct method to examine this hypothesis would be combined PET/microdialysis studies in nonhuman primates, which are confounded by the necessary anesthesia. Our results provide additional evidence supporting the idea that the GABA-shift phenomenon can be observed in vivo, using PET, in humans. The ability to measure in vivo changes in extracellular GABA levels provides a unique opportunity to explore the role of GABA in certain brain processes. Studies with nonhuman primates demonstrate that the disruption of GABA transmission in the DLFPC impairs working memory [54]. In humans, DLPFC gamma oscillations normally increase with working memory load [55], a phenomena which is impaired in subjects with working memory deficits [38]. In addition to playing a role in working memory [5], gamma synchrony appears to be associated with other higher cognitive processes such as associative learning [4]. Although the specific role of GABA transmission in working memory is still under investigation, the synchronization of pyramidal cell firing by networks of fast-spiking, parvalbumin-containing GABA neurons gives rise to oscillatory activity in the

gamma range [56]. While not powered to examine this issue specifically, in the current study, as in our previous one, we observed a relationship between the change in [^{11}C]flumazenil binding (in dose Group II) and the ability to entrain oscillatory activity in the gamma frequency during a cognitive control task. While in this study we only observed this relationship with one ROI, this provides further direct support for the hypothesis that GABA neurotransmission is linked to the synchronization of cortical neuronal activity in humans. Continued refinement and validation of the PET methodology described in this study is necessary for it to consistently provide the ability to measure changes in GABA levels in vivo; however, it provides a unique method to explore differences between control and patient populations in the degree of extracellular GABA increase in response to a standardized level of GAT1 blockade.

Acknowledgments

Author Contributions

Conceived and designed the experiments: WGF RYC DAL CAM RN. Performed the experiments: NSM CW. Analyzed the data: CMC MH. Wrote the paper: WGF RN.

References

1. Lutzenberger W, Pulvermuller F, Elbert T, Birbaumer N (1995) Visual stimulation alters local 40-Hz responses in humans: an EEG-study. Neuroscience Letters 183: 39–42.
2. Sanes J, Donoghue J (1993) Oscillations in Local Field Potentials of the Primate Motor Cortex During Voluntary Movement. PNAS 90: 4470–4474.
3. Tiitinen H, Sinkkonen J, Reinikainen K, Alho K, et al. (1993) Selective attention enhances the auditory 40-Hz transient response in humans. Nature Vol 364(6432, Jul 1993, 59–60 Nature Publishing Group, United Kingdom.
4. Miltner WHR, Braun C, Arnold M, Witte H, Taub E (1999) Coherence of gamma-band EEG activity as a basis for associative learning. Nature 397: 434–436.
5. Howard MW, Rizzuto DS, Caplan JB, Madsen JR, Lisman J, et al. (2003) Gamma Oscillations Correlate with Working Memory Load in Humans. Cerebral Cortex 13: 1369–1374.
6. Persson A, Ehrin E, Eriksson L, Farde L, Hedstrom CG, et al. (1985) Imaging of [11C]-labelled Ro 15-1788 binding to benzodiazepine receptors in the human brain by positron emission tomography. J Psychiatr Res 19: 609–622.
7. Frankle WG, Cho RY, Narendran R, Mason NS, Vora S, et al. (2009) Tiagabine increases [11C]flumazenil binding in cortical brain regions in healthy control subjects. Neuropsychopharmacology 34: 624–633.
8. Miller LG, Greenblatt DJ, Barnhill JG, Summer WR, Shader RI (1988) 'GABA shift' in vivo: enhancement of benzodiazepine binding in vivo by modulation of endogenous GABA. Eur J Pharmacol 148: 123–130.
9. Tallman JF, Thomas JW, Gallager DW (1978) GABAergic modulation of benzodiazepine binding site sensitivity. Nature 274: 383–385.
10. Braestrup C, Schmiechen R, Neef G, Nielsen M, Petersen EN (1982) Interaction of convulsive ligands with benzodiazepine receptors. Science 216: 1241–1243.
11. Bartos M, Vida I, Jonas P (2007) Synaptic mechanisms of synchronized gamma oscillations in inhibitory interneuron networks. Nat Rev Neurosci 8: 45–56.
12. Van Vreeswijk C, Abbott LF, Ermentrout GB (1994) When inhibition not excitation synchronizes neural firing. J Comput Neurosci 1: 313–321.
13. Mann EO, Suckling JM, Hajos N, Greenfield SA, Paulsen O (2005) Perisomatic feedback inhibition underlies cholinergically induced fast network oscillations in the rat hippocampus in vitro. Neuron 45: 105–117.
14. Hajos N, Palhalmi J, Mann EO, Nemeth B, Paulsen O, et al. (2004) Spike timing of distinct types of GABAergic interneuron during hippocampal gamma oscillations in vitro. J Neurosci 24: 9127–9137.
15. Fuchs EC, Zivkovic AR, Cunningham MO, Middleton S, Lebeau FE, et al. (2007) Recruitment of parvalbumin-positive interneurons determines hippocampal function and associated behavior. Neuron 53: 591–604.
16. Yoon JH, Maddock RJ, Rokem A, Silver MA, Minzenberg MJ, et al. (2010) GABA concentration is reduced in visual cortex in schizophrenia and correlates with orientation-specific surround suppression. The Journal of neuroscience : the official journal of the Society for Neuroscience 30: 3777–3781.
17. Price RB, Shungu DC, Mao X, Nestadt P, Kelly C, et al. (2009) Amino acid neurotransmitters assessed by proton magnetic resonance spectroscopy: relationship to treatment resistance in major depressive disorder. Biological Psychiatry 65: 792–800.
18. Halldin C, Stone-Enlander S, Thorell J-L, Persson A, Sedvall G (1988) 11C Labeling of Ro 15-1788 in two different positions, and also 11C labeling of its main metabolite Ro 15-3890, for PET studies of benzodiazepine receptors. Appl Radiat Isot 39: 993–997.
19. Barre L, Debruyne D, Abadie P, Moulin M, Baron JC (1991) A comparison of methods for separation of [11C]Ro 15-1788 (flumazenil) from its metabolites in the blood of rabbits, baboons, and humans. Appl Radiat Isot 42: 435–439.
20. Abi-Dargham A, Laruelle M, Seibyl J, Rattner Z, Baldwin RM, et al. (1994) SPECT measurement of benzodiazepine receptors in human brain with [123-I]iomazenil: kinetic and equilibrium paradigms. J Nucl Med 35: 228–238.
21. Price JC, Mayberg HS, Dannals RF, Wilson AA, Ravert HT, et al. (1993) Measurement of benzodiazepine receptor number and affinity in humans using tracer kinetic modeling, positron emission tomography, and [^{11}C]-flumazenil. J Cereb Blood Flow Metab 13: 656–667.
22. Zhang Y, Brady M, Smith S (2001) Segmentation of brain MR images through a hidden Markov random field model and the expectation-maximization algorithm. IEEE Trans Med Imaging 20: 45–57.
23. Smith SM, Jenkinson M, Woolrich MW, Beckmann CF, Behrens TE, et al. (2004) Advances in functional and structural MR image analysis and implementation as FSL. Neuroimage 23 Suppl 1: S208–219.
24. Watson C (2000) New, faster, image-based scatter correction for 3D PET. IEEE Trans Nucl Sci 47: 1587–1594.
25. Duvernoy H (1991) The human brain. Surface, three-dimensional sectional anatomy and MRI. New York: Sringer-Verlag Wien.
26. Talairach J, Tournoux P (1988) Co-planar stereotactic atlas of the human brain. Three-dimensional proportional system: an approach of cerebral imaging. New York: Thieme Medical Publisher.
27. Mintun MA, Raichle ME, Kilbourn MR, Wooten GF, Welch MJ (1984) A quantitative model for the in vivo assessment of drug binding sites with positron emission tomography. Ann Neurol 15: 217–227.
28. Innis R, Cunningham VJ, Delforge J, Fujioka K, Gjedde A, et al. (2007) Consensus nomenclature for in vivo imaging of reversibly binding radioligands. Journal of Cerebral Blood Flow and Metabolism 2007.
29. Innis RB, Cunningham VJ, Delforge J, Fujita M, Gjedde A, et al. (2007) Consensus nomenclature for in vivo imaging of reversibly binding radioligands. J Cereb Blood Flow Metab 27: 1533–1539.
30. Laruelle M, Baldwin RM, Rattner Z, Al-Tikriti MS, Zea-Ponce Y, et al. (1994) SPECT quantification of [123I]iomazenil binding to benzodiazepine receptors in nonhuman primates. I. Kinetic modeling of single bolus experiments. J Cereb Blood Flow Metab 14: 439–452.

31. Koeppe RA, Holthoff VA, Frey KA, Kilbourn MR, Kuhl DE (1991) Compartmental analysis of [^{11}C]flumazenil kinetics for the estimation of ligand transport rate and receptor distribution using positron emission tomography. J Cereb Blood Flow Metab 11: 735–744.

32. Levenberg K (1944) A method for the solution of certain problems in least squares. Quart Appl Math 2: 164–168.

33. Abadie P, Baron JC, Bisserbe JC, Boulenger JP, Rioux P, et al. (1992) Central benzodiazepine receptors in human brain: estimation of regional Bmax and KD values with positron emission tomography. Eur J Pharmacol 213: 107–115.

34. Möhler H, Okada T (1977) Benzodiazepine receptors: demonstration in the central nervous system. Science 198.

35. Braestrup C, Albrechten R, Squires RF (1977) High densities of benzodiazepine receptors in human cortical areas. Nature 269: 702–704.

36. Zezula J, Cortes R, Probst A, Palacios JM (1988) Benzodiazepine receptor sites in the human brain: autoradiographic mapping. Neuroscience 25: 771–795.

37. Lassen NA, Bartenstein PA, Lammertsma AA, Prevett MC, Turton DR, et al. (1995) Benzodiazepine receptor quantification in vivo in humans using [11C]flumazenil and PET: application of the steady-state principle. Journal of Cerebral Blood Flow & Metabolism 15: 152–165.

38. Cho RY, Konecky RO, Carter CS (2006) Impairments in frontal cortical gamma synchrony and cognitive control in schizophrenia. PNAS 103: 19878–19883.

39. Bertrand O, Perrin F, Pernier J (1985) A theoretical justification of the average reference in topographic evoked potential studies. Electroencephalogr Clin Neurophysiol 62: 462–464.

40. Adkins JC, Noble S (1998) Tiagabine. A review of its pharmacodynamic and pharmacokinetic properties and therapeutic potential in the management of epilepsy. Drugs 55: 437–460.

41. Uthman BM, Rowan AJ, Ahmann PA, Leppik IE, Schachter SC, et al. (1998) Tiagabine for complex partial seizures: a randomized, add-on, dose-response trial. Arch Neurol 55: 56–62.

42. During M, Mattson R, Scheyer R, Rask C, Pierce M, et al. The Effect of Tiagabine HCI on Extracellular GABA Levels in the Human Hippocampus. Annual Meeting of the American Epilepsy Society, 1992; Seattle, Washington.

43. Richards DA, Bowery NG (1996) Comparative effects of the GABA uptake inhibitors, tiagabine and NNC-711, on extracellular GABA levels in the rat ventrolateral thalamus. Neurochem Res 21: 135–140.

44. Fink-Jensen A, Suzdak PD, Swedberg MD, Judge ME, Hansen L, et al. (1992) The gamma-aminobutyric acid (GABA) uptake inhibitor, tiagabine, increases extracellular brain levels of GABA in awake rats. Eur J Pharmacol 220: 197–201.

45. Sybirska E, Seibyl JP, Bremner JD, Baldwin RM, al-Tikriti MS, et al. (1993) [123I]iomazenil SPECT imaging demonstrates significant benzodiazepine receptor reserve in human and nonhuman primate brain. Neuropharmacology 32: 671–680.

46. Mohler H, Richards JG (1981) Agonist and antagonist benzodiazepine receptor interaction in vitro. Nature 294: 763–765.

47. Rosenberg HC, Chiu TH (1979) Benzodiazepine binding after in vivo elevation of GABA. Neurosci Lett 15: 277–281.

48. Koe BK, Kondratas E, Russo LL (1987) [^{3}H]Ro 15-1788 binding to benzodiazepine receptors in mouse brain in vivo: marked enhancement by GABA agonists and other CNS drugs. European Journal of Pharmacology 142: 373–384.

49. Johannessen CU (2000) Mechanisms of action of valproate: a commentary. Neurochem Int 37: 103–110.

50. Belzung C, Le Guisquet AM, Crestani F (2000) Flumazenil induces benzodiazepine partial agonist-like effects in BALB/c but not C57BL/6 mice. Psychopharmacology 148: 24–32.

51. Kapczinski F, Curran HV, Gray J, Lader M (1994) Flumazenil has an anxiolytic effect in simulated stress. Psychopharmacology 114: 187–189.

52. Gerra G, Zaimovic A, Giusti F, Moi G, Brewer C (2002) Intravenous flumazenil versus oxazepam tapering in the treatment of benzodiazepine withdrawal: a randomized, placebo-controlled study. Addiction biology 7: 385–395.

53. Weiss M, Tikhonov D, Buldakova S (2002) Effect of flumazenil on GABAA receptors in isolated rat hippocampal neurons. Neurochemical research 27: 1605–1612.

54. Rao SG, Williams GV, Goldman-Rakic PS (2000) Destruction and creation of spatial tuning by disinhibition: GABA(A) blockade of prefrontal cortical neurons engaged by working memory. J Neurosci 20: 485–494.

55. Howard MW, Rizzuto DS, Caplan JB, Madsen JR, Lisman J, et al. (2003) Gamma oscillations correlate with working memory load in humans. Cereb Cortex 13: 1369–1374.

56. Sohal VS, Zhang F, Yizhar O, Deisseroth K (2009) Parvalbumin neurons and gamma rhythms enhance cortical circuit performance. Nature 459: 698–702.